ROYAL SOCIETY OF CHEMISTRY

PAPER

Check for updates

Computational investigation of multifunctional MOFs for adsorption and membrane-based separation of CF$_4$/CH$_4$, CH$_4$/H$_2$, CH$_4$/N$_2$, and N$_2$/H$_2$ mixtures†

Hakan Demir [ID] * and Seda Keskin [ID] *

The ease of functionalization of metal–organic frameworks (MOFs) can unlock unprecedented opportunities for gas adsorption and separation applications as the functional groups can impart favorable/ unfavorable regions/interactions for the desired/undesired adsorbates. In this study, the effects of the presence of multiple functional groups in MOFs on their CF$_4$/CH$_4$, CH$_4$/H$_2$, CH$_4$/N$_2$, and N$_2$/H$_2$ separation performances were computationally investigated combining grand canonical Monte Carlo (GCMC) and molecular dynamics (MD) simulations. The most promising adsorbents showing the best combinations of selectivity, working capacity, and regenerability were identified for each gas separation. 15, 13, and 16 out of the top 20 MOFs identified for the CH$_4$/H$_2$, CH$_4$/N$_2$, and N$_2$/H$_2$ adsorption-based separation, respectively, were found to have –OCH$_3$ groups as one of the functional groups. The biggest improvements in CF$_4$/CH$_4$, CH$_4$/H$_2$, CH$_4$/N$_2$, and N$_2$/H$_2$ selectivities were found to be induced by the presence of –OCH$_3$–OCH$_3$ groups in MOFs. For CH$_4$/H$_2$ separation, MOFs with two and three functionalized linkers were the best adsorbent candidates while for N$_2$/H$_2$ separation, all the top 20 materials involve two functional groups. Membrane performances of the MOFs were also studied for CH$_4$/ H$_2$ and CH$_4$/N$_2$ separation and the results showed that MOFs having –F–NH$_2$ and –F–OCH$_3$ functional groups present the highest separation performances considering both the membrane selectivity and permeability.

Design, System, Application

Metal–organic frameworks (MOFs) have appeared as promising candidates for various gas separations as they possess wider structural and chemical diversity than conventional materials such as activated carbon and zeolites. Thus far, many studies focused on the construction and/or testing of MOFs with single linker for gas separation applications. Multivariate MOFs (MTV-MOFs), which have multiple linker types, can supersede the gas separation performances of single-linker MOFs through synergistic effects of multiple linker types and/or functional groups. Here, a large collection of hypothetical MTV-MOFs, which involve different combinations of –F, –NH$_2$, and –OCH$_3$ groups, was computationally investigated to elucidate adsorption and membrane-based separation performances of materials for CF$_4$/CH$_4$, CH$_4$/H$_2$, CH$_4$/N$_2$, and N$_2$/H$_2$ mixtures. This work features not only the extents of performances of MTV-MOFs based on their functional groups but also determines the most favorable linker/functional group combinations for the gas separations of interest. Results of this work can guide the future experimental efforts on MOFs with the identified favorable linker/functional group combinations and accelerate the design and discovery of optimal materials for similar gas separations.

1. Introduction

The hybrid nature of metal–organic frameworks (MOFs), originating from their inorganic and organic constituents, has sparked much interest in their use for gas adsorption

and separation,[1,2] catalysis,[3] sensing,[4] and drug delivery[5] applications. MOFs have various structural features that can be highly beneficial for gas separation such as high surface area and porosity, tunable pore size/shape, and linker functionalization.[6,7] Given the large number of organic linker and metal node combinations and promising performances of MOFs, there is an increasing trend of designing and/or testing MOFs.[8–10]

MOFs have been tested for a wide variety of gas separations involving carbon capture, noble gas separation, hydrocarbon separation *etc.*[2] Among them, CF$_4$/CH$_4$ separation garnered less

Department of Chemical and Biological Engineering, Koc University, 34450 Istanbul, Turkey. E-mail: hakdemir@ku.edu.tr, skeskin@ku.edu.tr

† Electronic supplementary information (ESI) available. See DOI: https://doi.org/10.1039/d2me00130f

This journal is © The Royal Society of Chemistry and IChemE 2022

Mol. Syst. Des. Eng., 2022, 7, 1707–1721 | **1707**

interest despite the industrial CF_4 and CH_4 emission into the atmosphere, high global warming potential of CF_4 and its long atmospheric lifetime.[11–13] For example, Senkovska et al.[12] measured CF_4 adsorption in several porous materials at ambient conditions and reported the largest CF_4 uptake as 1.88 mol kg^{-1} in a MOF, $Zn_4O(dmcpz)_3$. Calero et al.[14] predicted CF_4 uptake in Cu-BTC to be around 1 mol kg^{-1} at ambient conditions using grand canonical Monte Carlo (GCMC) simulations. Our earlier work[15] focused on a collection of Zr-MOFs and reported CF_4/CH_4 selectivity, CF_4 working capacity, and CF_4 regenerability to vary in the ranges of 0.8–6.2, 0.3–2.1 mol kg^{-1}, and 54.0–89.9%, respectively.

Due to the cleaner combustion characteristics of CH_4 compared to gasoline and newly discovered reserves, it has become a more preferred energy source to reduce CO_2 concentration in the air.[16] Similarly, the combustion of H_2 ideally leads to no harmful emission whose widespread use can play a significant role in environmental remediation.[17,18] It is known that CH_4 steam reforming and dry reforming lead to a gas mixture involving CH_4 and H_2.[19,20] As the efficient separation of CH_4/H_2 mixture can result in two sources of fuels that would be more preferable than the conventional fossil fuels, much research has been done on developing and identifying favorable materials for the CH_4/H_2 separation.[21,22] High-throughput computational screening of 4350 and 4240 MOFs for adsorption and membrane-based separation of CH_4/H_2 showed that MOFs can potentially have higher CH_4/H_2 adsorption selectivity (up to 2028), CH_4 working capacities (up to 7.3 mol kg^{-1}), CH_4/H_2 membrane selectivity (up to 713), and CH_4 permeability (up to 1.2×10^8 Barrer) than zeolites.[23,24]

CH_4 and N_2 can co-exist in shale gases, natural gases, and landfill gases whose separation through conventional methods is energetically inefficient.[25] CH_4/N_2 separation performances of MOFs have been experimentally probed in several studies and the ideal CH_4/N_2 selectivities at ambient temperature were found to vary from 1.4 to 8.3.[26–28] Sumer et al.[29] screened more than 100 MOFs for CH_4/N_2 separation and the best adsorbent was found to have a CH_4/N_2 selectivity of 6.71 at 10 bar, 298 K, and CH_4 working capacity of 3.64 mol kg^{-1} (between 10 and 1 bar). The top adsorbent has also been reported as one of the top materials for the membrane-based separation with a CH_4/N_2 membrane selectivity of 10.26 and CH_4 permeability of 2.61×10^6 Barrer. Yan et al.[30] performed a high-throughput computational screening of >300 000 MOFs for separation of equimolar CH_4/N_2 (50/50) separation at ambient conditions and the highest CH_4/N_2 selectivity was reported as 29.5. Gulbalkan et al.[31] recently screened a large collection of MOFs and covalent-organic frameworks (COFs) composed of 5034 materials for CH_4/N_2 separation at pressure-swing adsorption operation conditions and the highest CH_4/N_2 selectivity was around 14.

N_2/H_2 separation is one of the less investigated gas separations while N_2 and H_2 uptakes of MOFs are more commonly reported. For instance, Mu et al.[32] synthesized UMCM-1 and obtained its maximum H_2 storage capacity at 298 K, 26 bar as 3.4 mol kg^{-1} in addition to a N_2 uptake of ~4 mol kg^{-1} at 298 K, 25 bar. In an experimental study by Moreira et al.,[16] it has been shown that UiO-66(Zr)–$(COOH)_2$ exhibits a higher affinity towards N_2 than H_2 at 269–373 K over a wide pressure range up to 30 bar (N_2/H_2 ideal selectivity of ~8 at 269 K, 20 bar). Regufe et al.[33] measured N_2 and H_2 adsorption in MIL-125(Ti)–NH_2 at 303 K from which it was concluded that N_2 affinity of the material is greater than H_2 affinity (N_2/H_2 ideal selectivity of ~1.3 at 303 K, 1 bar). Azar et al.[34] performed a large-scale computational screening of MOFs for adsorption-based H_2/N_2 separation at ambient conditions and reported H_2/N_2 selectivities of ~0.01–0.7 implying that all MOFs were N_2 selective.

Many of the MOF studies in the literature focus on single-linker MOFs some of which have shown superior performances than conventional materials as outlined above. Besides single-linker MOFs, multivariate (MTV)-MOFs can also serve as efficient gas separation platforms as the combination of multiple functionalized linkers can lead to tailored gas affinities and significantly enhanced gas separation performances compared to pristine MOFs.[35,36] MTV-MOFs can be more selective than their counterparts with single type of functionalization. For instance, an MTV-MOF based on the functionalization of UiO-66 with –NH_2 and –F_4 groups has been predicted to have higher CO_2/N_2 selectivities (26.3) than UiO-66 structures with solely –NH_2 or –F_4 functionalization (24.9 and 6.4).[37] Thus, unlocking the gas separation performance of MTV-MOFs for adsorption and membrane-based gas separations is highly desired.

In this work, MTV-MOFs[38] were computationally studied using a multi-stage screening procedure, mainly involving structural filtering and GCMC simulations, to investigate their potential for adsorption-based separation of CF_4/CH_4, CH_4/H_2, CH_4/N_2, and N_2/H_2 mixtures. The investigated MTV-MOF database involves bare MOFs and their functionalized counterparts which may include up to three different functional groups (–F, –NH_2, –OCH_3) constituting 16 subgroups of MTV-MOFs (e.g., –F–NH_2–OCH_3). For each MOF, gas uptakes were computed using GCMC simulations and these results were used to calculate adsorption selectivity, working capacity, and regenerability and based on the combination of these metrics, the top MOF adsorbents were identified. Besides, high-performing MOF adsorbents were further studied for membrane-based CH_4/H_2 and CH_4/N_2 separations. After identifying the top adsorbent and membranes materials for each gas separation, we examined structure-performance relations and discussed which combination of functional groups can lead to favorable adsorption and membrane-based separation performances of MOFs. As the subgroups of MTV-MOFs involve not only cases having two or three different functional groups but also linkers with identical functional groups, our results reveal the potential separation performance gains by grafting identical or disparate functional groups.

1708 | Mol. Syst. Des. Eng., 2022, **7**, 1707–1721

This journal is © The Royal Society of Chemistry and IChemE 2022
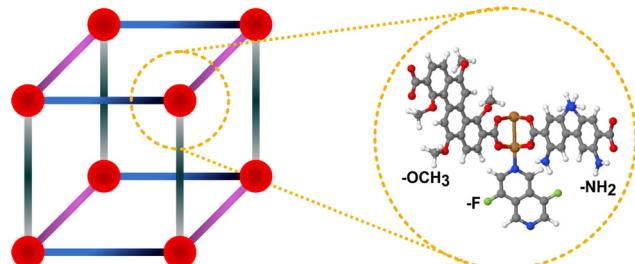
Fig. 1 Typical structures of MTV-MOFs probed (left) and a section of a representative MTV-MOF having three different functionalities (right) (different colourings of linkers on the left designate different linkers which may have different functional groups. Atom colouring: gray: C, red: O, brown: Cu, green: F, white: H, blue: N).

2. Computational methods

In this work, we focused on the MTV-MOF database[38] (based on copper paddlewheel nodes and pcu topology) involving 560 parent/bare MOFs (structures originally named as pMOFs) and 10995 functionalized MOFs (structures originally named as cuf MOFs). The functionalized MOFs may include –F, –NH$_2$, and/or –OCH$_3$ functional groups. Fig. 1 demonstrates the general structures of MTV-MOFs as well as an example MTV-MOF where each linker involves different functional group (–F, –NH$_2$ and –OCH$_3$). The textural properties of 11129 MOFs (GCD (global cavity diameter), PLD (pore limiting diameter), LCD (largest cavity diameter), surface area, probe-occupiable void fraction, probe-occupiable pore volume) were calculated with a probe radius of 1.84 Å using Zeo++.[39,40] Note that GCD is the largest pore size in the material which may not be found in the pore channel where PLD and LCD are located.[41] Fig. 2 demonstrates the structural property distributions of all MTV-MOFs except those having too close interatomic distances (*i.e.*, interatomic distances less than 0.9 Å). It can be inferred that the MTV-MOF database involves structurally diverse structures where bare MOFs are somewhat more porous than their functionalized counterparts. The PLD distribution curves overlap in a large range of values while the discrepancies in surface area, void fraction, and pore volume distributions are considerably larger.

MOFs that satisfy the following criteria were kept for further molecular simulations to eliminate potential structural accessibility, structural integrity, and practical use problems: (1) MOFs shall have non-zero accessible surface areas and PLDs larger than sizes of adsorbates that are of interest ensuring structural accessibility. (2) Interatomic distances in MOFs shall be larger than 0.9 Å to avoid structures with atomic overlaps or too close atoms. (3) Working capacities, the differences between gas uptakes computed at adsorption and desorption conditions, shall be positive to have practical use of MOFs in pressure/vacuum swing adsorption operations. After applying these criteria, we ended up with 11035, 11115, 11115, and 11116 different MOFs for the separation of CF$_4$/CH$_4$, CH$_4$/H$_2$, CH$_4$/N$_2$, and N$_2$/H$_2$ mixtures.

Adsorption of CF$_4$/CH$_4$, CH$_4$/H$_2$, CH$_4$/N$_2$, and N$_2$/H$_2$ mixtures in MTV MOFs was investigated using GCMC simulations and diffusion of CH$_4$/H$_2$ and CH$_4$/N$_2$ mixtures in MTV-MOFs were studied by molecular dynamics (MD) simulations in RASPA, respectively.[42] Bulk compositions of these gas mixtures were determined such that they have industrial relevance and/or enable benchmark with other
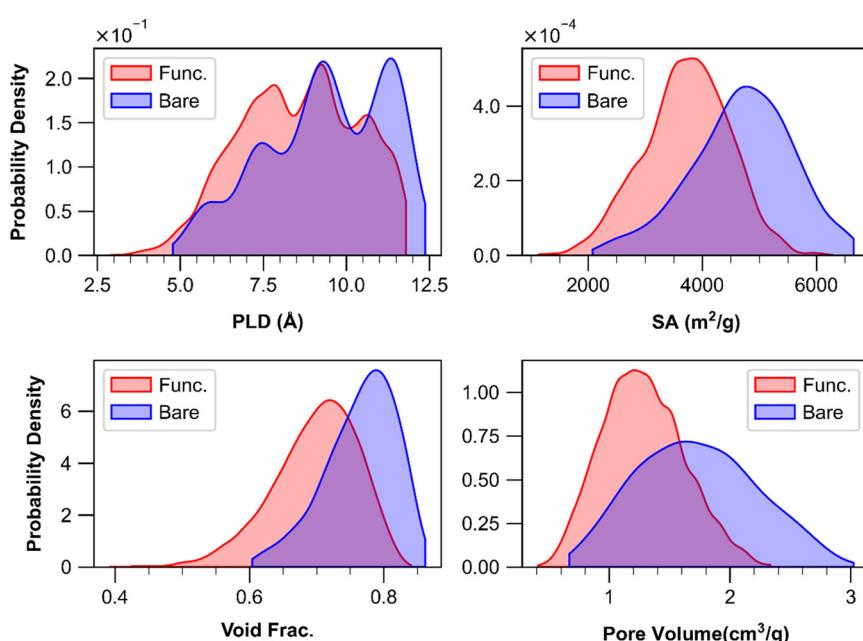
Fig. 2 Kernel density plots showing distribution of structural properties of 11129 MTV-MOFs where bare and functionalized (Func.) MOFs were shown separately.

literature studies.[24,31,43,44] For instance, CF_4 removal from CH_4 constitutes a significant stage of reducing greenhouse gas concentration in the air.[15] As these two sorbates have similar properties, finding sorbents that can achieve efficient CF_4/CH_4 separation is crucial. While a large variety of gas compositions has been studied earlier for CF_4/CH_4 separation,[43] we preferred an equimolar mixture to be able to benchmark the results of this work with our earlier work[15] which was possibly the largest MOF screening work in terms of CF_4/CH_4 separation. H_2 or N_2 removal from CH_4 is highly important in the context of natural gas separation for which equimolar binary mixtures are typically used.[31,45] Similarly, improving the efficiency of N_2/H_2 separation bears importance for the processes of carbon black manufacturing, and ammonia synthesis.[46,47] N_2/H_2 composition is selected based on former experimental and computational studies.[34,48] These gas compositions and pressures were listed in Table S1† together with total simulation cycles for GCMC. All GCMC simulations were carried out at 298 K. In all GCMC simulations, the number of equilibration and production cycles were equal. The following types of moves were employed with equal probability: insertion/deletion, translation, rotation (only for N_2), and molecule identity change. MOF atoms were assigned Universal Force Field (UFF[49]) parameters and partial atomic charges in metal–organic frameworks (PACMOF[50]) charges. The interaction parameters for the gas molecules were obtained from the literature which are available in Table S2.†[51–54] The Lennard–Jones interactions were cutoff at 12 Å and electrostatic calculations were performed (only for N_2) using Ewald summation method.[55]

Results of GCMC simulations, the adsorbed gas amounts (N_i), were used to compute the adsorption-based gas separation performances of MOFs: the adsorption selectivity is defined as $S_{ads1/2} = \frac{N_1/N_2}{y_1/y_2}$ where N and y designate the adsorption amount and the mole fraction of a gas component in the mixture. Working capacity is mathematically expressed as $\Delta N_1 = N_{ads,1} - \Delta N_{des,1}$ where the first and second term on the right-hand side represent gas uptakes computed from GCMC simulations at the adsorption and desorption conditions. Regenerability of an adsorbent is calculated as $R = \frac{\Delta N_1}{N_{ads,1}} \times 100$.[66] Since all of these metrics, selectivity, working capacity and regenerability, are important to identify the most promising MOF adsorbents, we defined the $Score_{X,i} = \frac{X_i}{X_{max}} \times 100$, where X_i and X_{max} denote the value of the individual performance metric X (selectivity/ working capacity/regenerability) for material i and the highest value of the individual performance metric X across all materials, respectively. The individual separation performance scores were summed to determine the overall separation performance scores of MOFs and the materials with the highest overall separation performances were assigned the highest adsorbent rankings.

For the top materials identified for each gas separation, MD simulations were performed in the NVT ensemble at 298 K using a Nose–Hoover thermostat.[56] In these simulations, 10^5 initialization, 10^6 equilibration, and 15×10^6 production steps (time step of 1 fs) were used where the number of gas molecules (gas loading) employed relies on GCMC simulation results at adsorption conditions. Self-diffusivities of gases in x, y, and z directions were determined using Einstein's relation at long simulation times.[57] Self-diffusivities in a particular direction that were much lower (e.g., two orders of magnitude smaller) than other self-diffusivities in other directions were discarded in the calculation of average self-diffusivity calculation $\left(D_{self,i} = \frac{D_{self,i,x} + D_{self,i,y} + D_{self,i,z}}{3} \right)$. In such cases, the dimensionality of the system in Einstein's relation was adjusted accordingly. The self-diffusivities are averaged over five simulations. Combining the results of GCMC and MD simulations, gas permeabilities were calculated as $P_i = \frac{c_i \times D_{self,i}}{f_i}$ where c_i, $D_{self,i}$, and f_i represent the gas concentration at the feed side, self-diffusivity of gas, and feed side fugacity of the gas species i, respectively. The diffusion selectivity and membrane selectivity (component 1 over 2) are defined as $S_{diff,12} = \frac{D_{self,1}}{D_{self,2}}$ and $S_{mem,12} = S_{ads,12} \times S_{diff,12}$, successively.[66]

3. Results & discussion

3.1 CF_4/CH_4 separation

Fig. S1† delineates the CF_4/CH_4 separation performance metrics of 11 035 MOFs as well as their pore features. The top left panel shows CF_4/CH_4 selectivity, CF_4 working capacity, and CF_4 regenerability of the MOFs which were calculated as 1.4–8.2, 0.2–2.9 mol kg^{-1}, and 45.9–90.5%, respectively. The three most CF_4 selective MOFs (pMOF_10, cuf_3865, and cuf_8464) exhibit CF_4/CH_4 selectivities of 8.2, 7.8, and 7.8, CF_4 working capacities of 2.9, 2.4, and 1.6 mol kg^{-1}, and CF_4 regenerabilities of 71.6, 70.2, and 64.9%, respectively. The top right panel shows that there is a group of highly porous MOFs (void fraction mostly >0.7) located in the relatively low CF_4/CH_4 selectivity (<4) and CF_4 working capacity range (<1 mol kg^{-1}). In contrast, MOFs with the highest CF_4/CH_4 selectivity and CF_4 working capacity possess medium-high void fractions (~0.46–0.68). The bottom left panel exhibits that the most CF_4 selective MOFs have PLDs of ~6 Å. However, there are also MOFs with similar PLDs attaining very low selectivities (<2). The bottom right panel illustrates that the largest CF_4/CH_4 selectivities are located around 2000 m^2 g^{-1} whereas the smallest CF_4/CH_4 selectivities are obtained by MOFs with very large surface areas (>5000 m^2 g^{-1}). All in all, these results suggest that MTV-MOFs that are not overly porous (i.e., PLDs <7 Å, surface areas <3000 m^2 g^{-1}) can attain high adsorption-based CF_4/CH_4 separation performances in terms of selectivity, working capacity, and regenerability.

Fig. 3 shows the breakdown of CF_4/CH_4 separation performance metrics and textural features of MOFs into functional groups. The top left panel exhibits that, on average, MOFs having linkers functionalized with $-OCH_3$ groups (specifically, $-OCH_3-OCH_3$, meaning two linkers are functionalized with $-OCH_3$ group) are the most CF_4 selective. On the contrary, those functionalized with $-F$ groups (i.e., $-F-$

1710 | Mol. Syst. Des. Eng., 2022, 7, 1707–1721

This journal is © The Royal Society of Chemistry and IChemE 2022
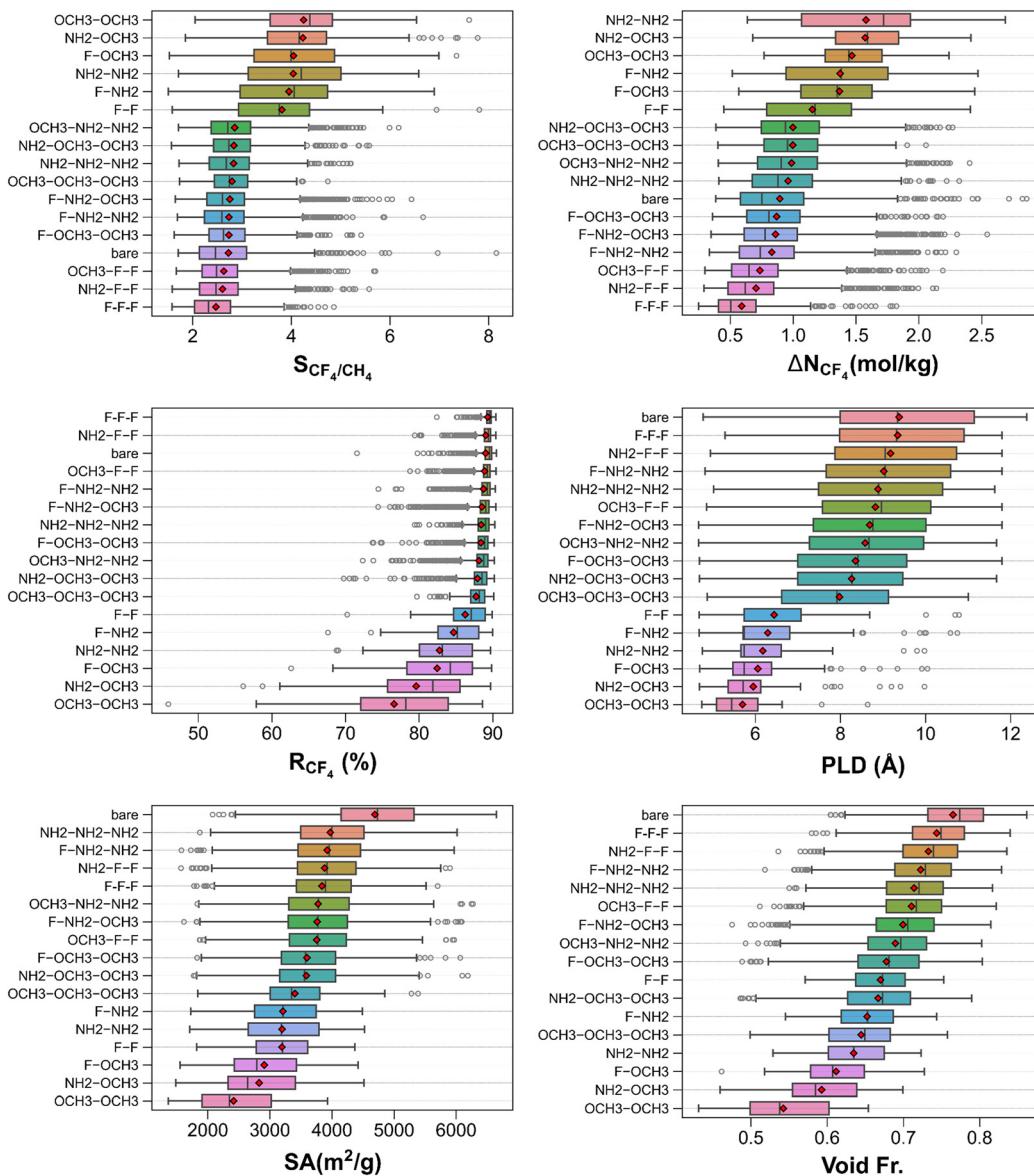
Fig. 3 CF_4/CH_4 separation performance metrics of MTV MOFs and their pore features categorized by their functional groups. In all box-and-whisker plots, MOF groups are sorted from top to bottom by mean values in descending order where mean values are shown with red diamonds. Boxes show the range of values between the first and third quartile while the whiskers designate the distribution of other data points except outliers. Outliers are denoted as empty circles which are defined as data points away from either end of the boxes by more than 1.5 interquartile range.

F–F) are the least CF_4 selective. Bare MOFs is one of the groups showing large variations in selectivity from 1.7 up to 8.2. In general, the lowest CF_4/CH_4 selectivity obtained in each group is very close to each other suggesting that there are cases where the selectivity of the bare MOFs may not be simply improved through functionalization. The top right panel depicts that MOFs functionalized with $-NH_2-NH_2$ (–F–F–F) groups attain the largest (smallest) mean CF_4 working capacities. As a group, bare MOFs attain one of the low mean CF_4 working capacities ($\sim$0.9 mol kg^{-1}), however, some MOFs among them can demonstrate quite high working capacities as exemplified by pMOF_10 with the highest CF_4 working capacity of 2.9 mol kg^{-1}. The middle-left panel illustrates that many groups of MOFs (going from top to bottom, –F–F–F to

$-OCH_3-OCH_3-OCH_3$) show high CF_4 regenerabilities ($>$85%). In contrast, MOFs functionalized with $-OCH_3-OCH_3$ and $-NH_2-OCH_3$ groups acquire the lowest mean CF_4 regenerabilities ($<$80%). Overall, these observations imply that by combining multiple functional groups, CF_4/CH_4 separation performance metrics of MOFs can be drastically altered. However, this does not guarantee that multifunctional MOFs can always perform better than all bare MOFs in terms of a particular separation performance metric.

Since the grafting of functional groups can block portions of the pores or create new surfaces, the textural properties of bare and functionalized MOFs are benchmarked to see if there are clear pore feature trends across different groups of

MOFs. As the middle right panel demonstrates, several categories of MOFs (bare MOFs, MOFs functionalized with –F –F–F and –NH$_2$–F–F groups) possess very similar and high PLDs on average. The smallest PLDs belong to MOFs that are functionalized with –OCH$_3$–OCH$_3$ groups. The bottom panels show that the bare MOFs possess the highest mean surface area and void fraction whereas MOFs functionalized with –OCH$_3$–OCH$_3$ groups have the lowest mean surface areas, in line with the PLD trends.

Unlike the traditional approach of ranking materials solely based on adsorption selectivities, here, we evaluated MOF adsorbents using multiple metrics (*i.e.*, adsorption selectivity, working capacity, and regenerability). Table S3† enumerates the 20 best performing MOFs identified for adsorption-based separation of CF$_4$/CH$_4$ mixture. These MOFs are dominantly

functionalized MOFs (16 out of 20), yet the top three MOFs are all bare MOFs (pMOF_10, pMOF_26, and pMOF_8) with CF$_4$/CH$_4$ selectivities of 6.0–8.2, CF$_4$ working capacities of 2.7–2.9 mol kg^{-1}, and CF$_4$ regenerabilities of 71.6–80.6%. Considering the number of occurrences in the top 20 list, –F–NH$_2$ functionalization is one of the cases which achieve favorable CF$_4$/CH$_4$ separation features. It is noteworthy that most of these top MOFs possess narrow pores (~5–7 Å) with surface areas of 1824.7–3724.8 m^2 g^{-1}, void fractions of 0.496–0.657, and pore volumes of 0.574–0.941 cm^3 g^{-1}.

3.2 CH$_4$/H$_2$ separation

Fig. S2† shows CH$_4$/H$_2$ separation performance metrics of the MOFs together with their textural properties. As the top left
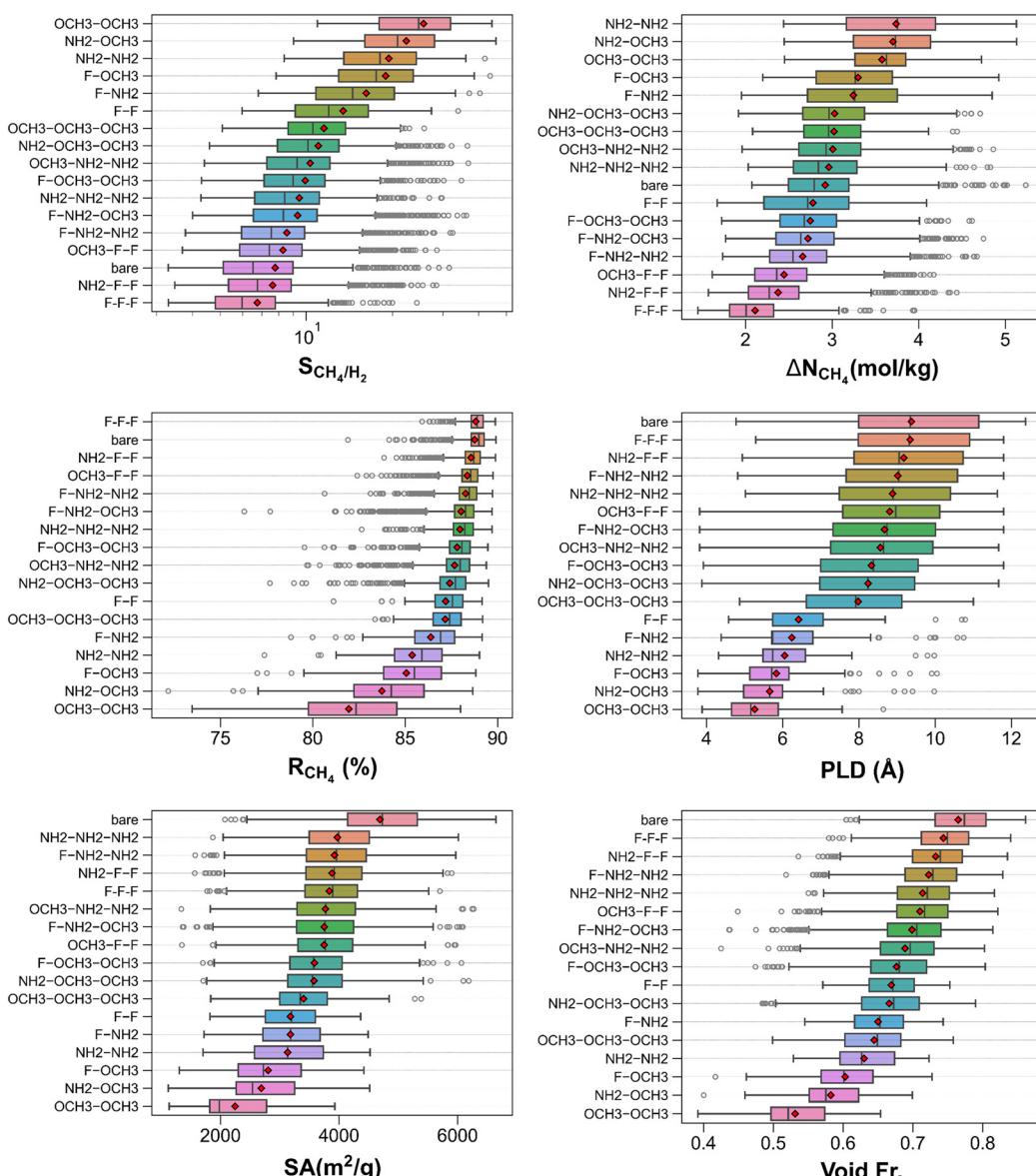
Fig. 4 CH$_4$/H$_2$ separation performance metrics and structural properties of MOFs classified by their functional groups.

1712 | *Mol. Syst. Des. Eng.*, 2022, **7**, 1707–1721

This journal is © The Royal Society of Chemistry and IChemE 2022

panel demonstrates, most of the MOFs are highly regenerable (CH_4 regenerability >85%). CH_4/H_2 selectivity and CH_4 working capacity of the MOFs span the ranges of 3.3–46.0, and 1.5–5.2 mol kg^{-1}, respectively. The top right panel exhibits that more CH_4 selective MOFs tend to be denser than less CH_4 selective ones. Interestingly, the most porous structures (void fraction $\gtrsim$0.85) attain limited CH_4 working capacities (<2.4 mol kg^{-1}) whereas MOFs with the largest CH_4 working capacities possess medium-high void fractions (0.56–0.67). The bottom panels illustrate the clear inverse CH_4/H_2 selectivity *vs.* PLD and CH_4/H_2 selectivity *vs.* surface area trends where the highest selectivities are attained around PLDs of 4–6 Å and surface areas of ~1200–2200 m^2 g^{-1}. Since both adsorbates interact with the framework through dispersion forces only, these inverse trends hint the significantly reduced dispersion effects as the structure become more porous. Thus, superior CH_4/H_2 separation performances are more likely to found in MTV-MOFs with relatively small pores and porosities.

Fig. 4 displays the classification of the CH_4/H_2 separation performance metrics and structural features of the MOFs by functional groups. The top left panel shows that the most (least) CH_4 selective MOFs are $-OCH_3-OCH_3$ ($-F-F-F$) functionalized MOFs on average. While bare MOFs tend to have lower CH_4/H_2 selectivities than some of the functionalized MOF groups (such as $-OCH_3-OCH_3$, $-NH_2-OCH_3$, and $-NH_2-NH_2$), some of the bare MOFs can have high CH_4/H_2 selectivities (up to ~32), comparable with most of the functionalized MOFs. The top right panel exhibits that both bare and functionalized MOFs can span large ranges of CH_4 working capacities. Interestingly, the largest CH_4 working capacities are obtained by the MOFs functionalized with three functional groups (*i.e.*, $-OCH_3-NH_2-NH_2$, and $-NH_2-NH_2-NH_2$) despite reduced space for adsorption. The

middle-left panel shows that many groups of MOFs exhibit similar CH_4 regenerabilities on average (>85%) while those functionalized with $-OCH_3-OCH_3$ have the most dissimilar mean CH_4 regenerability (~82%), being the lowest. Considering all above, it can be inferred that addition of multiple functional groups modifies the pore structures dramatically which in turn can bring about significantly different CH_4/H_2 adsorption-based separation performances.

Table 1 lists the top 20 MOFs identified for CH_4/H_2 separation and they are all found to be functionalized structures. The best three MOFs are cuf_2878, cuf_824, and cuf_818 with CH_4/H_2 selectivities of 42.1, 46.0, and 43.9, CH_4 working capacities of 5.1, 4.6, and 4.6 mol kg^{-1}, and CH_4 regenerabilities of 80.3, 76.2, and 77.5%, respectively. As many other materials in the top 20 list are, these top materials are also functionalized with $-NH_2$ group (*i.e.*, $-NH_2-OCH_3$, $-OCH_3-NH_2-NH_2$, and $-NH_2-NH_2$, respectively) (see Table S4†). Considering the ranges of PLD (3.94–6.37 Å), surface area (1136.1–2543.9 m^2 g^{-1}), void fraction (0.437–0.581), and pore volume (0.455–0.712 cm^3 g^{-1}), the top 20 MOFs can be regarded as moderately porous structures (see Table S4†).

While porous materials can serve as adsorbents in separation processes, they can also act as efficient membranes as long as adsorbates diffuse fast enough through the pores of the material. It is known that the computational cost of obtaining membrane-based performances is much higher than that of adsorption-based performances.[67] Thus, we chose only two cases (CH_4/H_2 and CH_4/N_2), which are the most commonly studied cases among all four cases, to investigate membrane-based separation. To reveal the potential of MTV-MOFs as membranes, MD calculations were performed for the top 20 adsorbents to compute the diffusion of CH_4/H_2 and CH_4/N_2 mixture in the pores. As expected, H_2 diffuses faster than CH_4

Table 1 20 best performing MOF adsorbents for the CH_4/H_2 separation together with their membrane-based separation performances

Structure	$S_{ads,CH_4/H_2}$	ΔN_{CH_4} (mol kg^{-1})	R_{CH_4} (%)	$S_{diff,CH_4/H_2}$	$S_{mem,CH_4/H_2}$	D_{self,CH_4} (m^2 s^{-1})	D_{self,H_2} (m^2 s^{-1})	P_{CH_4} (Barrer)	P_{H_2} (Barrer)
cuf_2878	42.1	5.1	80.3	0.24	10.0	1.40×10^{-8}	5.92×10^{-8}	4.77×10^5	4.67×10^4
cuf_824	46.0	4.6	76.2	0.24	10.9	1.24×10^{-8}	5.22×10^{-8}	4.27×10^5	3.83×10^4
cuf_818	43.9	4.6	77.5	0.28	12.2	1.98×10^{-8}	7.13×10^{-8}	6.78×10^5	5.44×10^4
cuf_586	37.8	5.0	80.2	0.27	10.2	1.15×10^{-8}	4.27×10^{-8}	3.82×10^5	3.65×10^4
cuf_110	42.2	4.7	75.2	0.15	6.2	5.25×10^{-9}	3.59×10^{-8}	1.75×10^5	2.77×10^4
cuf_3153	42.3	4.5	78.5	0.18	7.5	3.86×10^{-9}	2.19×10^{-8}	1.24×10^5	1.62×10^4
cuf_1627	38.2	4.7	81.9	0.29	11.2	1.77×10^{-8}	6.03×10^{-8}	5.55×10^5	4.82×10^4
cuf_2872	37.1	4.8	81.2	0.29	10.7	2.23×10^{-8}	7.73×10^{-8}	7.11×10^5	6.49×10^4
cuf_7134	42.6	4.3	78.8	0.29	12.4	1.22×10^{-8}	4.20×10^{-8}	3.89×10^5	3.07×10^4
cuf_1633	39.1	4.5	79.9	0.24	9.4	1.22×10^{-8}	5.11×10^{-8}	3.77×10^5	3.93×10^4
cuf_3160	38.7	4.5	80.7	0.18	7.1	4.54×10^{-9}	2.47×10^{-8}	1.44×10^5	1.99×10^4
cuf_3866	40.4	4.4	78.8	0.34	13.6	2.07×10^{-8}	6.15×10^{-8}	6.97×10^5	4.99×10^4
cuf_2640	32.8	5.0	81.3	0.25	8.3	1.47×10^{-8}	5.82×10^{-8}	4.50×10^5	5.28×10^4
cuf_810	36.5	4.6	80.9	0.21	7.6	7.98×10^{-9}	3.84×10^{-8}	2.52×10^5	3.24×10^4
cuf_2160	35.1	4.9	78.9	0.11	3.8	4.87×10^{-9}	4.54×10^{-8}	1.51×10^5	3.90×10^4
cuf_533	35.0	4.7	80.9	0.24	8.4	1.88×10^{-8}	7.84×10^{-8}	5.90×10^5	6.85×10^4
cuf_811	34.8	4.6	82.1	0.21	7.3	1.13×10^{-8}	5.37×10^{-8}	3.52×10^5	4.69×10^4
cuf_3143	44.5	3.8	75.0	0.10	4.3	1.30×10^{-8}	1.34×10^{-8}	3.89×10^4	8.75×10^3
cuf_812	42.1	4.0	75.9	0.13	5.6	4.54×10^{-9}	3.43×10^{-8}	1.43×10^5	2.51×10^4
cuf_9626	34.3	4.6	81.6	0.24	8.2	9.41×10^{-9}	3.92×10^{-8}	2.91×10^5	3.45×10^4

This journal is © The Royal Society of Chemistry and IChemE 2022

Mol. Syst. Des. Eng., 2022, **7**, 1707–1721 | **1713**

since it has weaker interaction with the MOF atoms compared to CH_4 in addition to being lighter and smaller. This leads to CH_4/H_2 diffusion selectivities that are considerably smaller than unity for all the MTV-MOFs that we studied by MD. Combining the low diffusion selectivities toward CH_4 with the high adsorption selectivities lead to membranes offering CH_4/H_2 membrane selectivities in the range of ~4–14. Weighing CH_4/H_2 membrane selectivity and CH_4 permeability equally for identifying the best membrane materials, cuf_3866 (F–NH_2 functionalized), cuf_818 (F–OCH_3 functionalized), and cuf_2872 (F–NH_2 functionalized) were found to be the ideal candidates for the selective CH_4 removal from H_2 with CH_4/H_2 membrane selectivities of 10.7–13.6 and CH_4 permeabilities of 6.78×10^5–7.11×10^5 Barrer. CH_4 permeabilities are generally about one order of magnitude larger than H_2 permeabilities which is largely due to the stronger adsorption of CH_4 compared to H_2 (higher concentrations of CH_4 in the membrane).

3.3 CH_4/N_2 separation

Fig. S3† delineates the CH_4/N_2 separation performance metrics of the MOFs along with their textural properties. The top left panel demonstrates that the CH_4/N_2 selectivities, CH_4 working capacities, and CH_4 regenerabilities cover the ranges of 1.4–5.2, 1.4–4.8 mol kg^{-1}, and 69.9–89.7%, respectively. While the two most CH_4 selective MOFs can attain somewhat higher CH_4/N_2 selectivities (>5) than the rest of the material set, they suffer from relatively low regenerability (<75%), signifying a trade-off between the selectivity and reusability of materials. The top right panel shows that high CH_4/N_2 selectivities (>4) are seen in moderately porous structures (void fraction of 0.392–0.636) while the most porous structures (void fraction >0.84) can acquire CH_4/N_2 selectivities up to 1.7 and CH_4 working capacities up to 2.3 mol kg^{-1}. The bottom panels reveal that the biggest spreads

Fig. 5 Breakdown of CH_4/N_2 separation performance metrics and textural properties of MOFs.

1714 | *Mol. Syst. Des. Eng.*, 2022, **7**, 1707–1721

This journal is © The Royal Society of Chemistry and IChemE 2022

in CH_4/N_2 selectivity are observed at relatively low PLDs ($\sim$6 Å) and surface areas ($\sim$2000 m^2 g^{-1}) beyond which selectivities start converging to 2–3. Comparing Fig. S2 and S3,† it can be deduced that the separation performances trends seen for the CH_4/H_2 and CH_4/N_2 adsorption-based separation are very similar to each other albeit MTV-MOFs having smaller CH_4/N_2 adsorption selectivities as N_2, having a quadrupole moment, interacts slightly stronger than H_2.

Fig. 5 displays the categorized (by functional groups) CH_4/N_2 separation performance metrics and textural properties of MOFs. The top left panel shows that while –NH_2–OCH_3 and –F–OCH_3 functionalized MOFs can achieve large CH_4/N_2 selectivities, the highest mean CH_4/N_2 selectivities are obtained by the MOFs functionalized with –OCH_3–OCH_3. The mean CH_4/N_2 selectivity of bare MOFs is one of the lowest of all groups below which MOFs functionalized with –NH_2–F–F and –F–F–F are located with slightly lower mean selectivities. The top right panel demonstrates that the largest (smallest) mean CH_4 working capacity is attained by MOFs functionalized with –NH_2–NH_2 (–F–F–F). However, the largest CH_4 working capacity was observed in a bare MOF. The middle-left panel manifests that many functionalized MOF groups (e.g., –F–F–F, –NH_2–F–F, –OCH_3–F–F etc.) and bare MOFs acquire similarly high CH_4 regenerabilities on average ($>$85%) while MOFs functionalized with –OCH_3–OCH_3 have the least mean CH_4 regenerability ($\sim$80%) which is comparable with the former.

In Table 2, 20 best performing MOFs for CH_4/N_2 separation are tabulated where CH_4/N_2 selectivities, CH_4 working capacities, and CH_4 regenerabilities span the ranges of 3.5–5.0, 3.8–4.8 mol kg^{-1}, and 73.0–84.6%, respectively. These MOFs are moderately porous structures with PLDs of 4.09–11.39 Å, surface areas of 1868.0–3277.6 m^2 g^{-1}, void fractions of 0.514–0.650, and pore volumes of 0.557–0.937 cm^3 g^{-1} (see

Table S5†). Among the top 20 MOFs, which are all functionalized MOFs, the top three MOFs (cuf_2878, cuf_1627, and cuf_586) are functionalized with –F, –OCH_3 and –NH_2 groups (i.e., –NH_2–NH_2, –F–OCH_3, and –NH_2–OCH_3, successively) (see Table S5†). While they attain moderate-high selectivities (4.6, 4.7, and 4.5), they exhibit large CH_4 working capacities (4.5, 4.2, and 4.4 mol kg^{-1}) together with high CH_4 regenerabilities (78.5, 80.4, and 78.5%).

Table 2 lists the membrane-based separation performances of top 20 MOF adsorbents for CH_4/N_2 separation where they show similar performances in terms of membrane selectivity and CH_4 permeability. Considering CH_4/N_2 membrane selectivity and CH_4 permeability in equal weight, cuf_818 (F–OCH_3 functionalized), cuf_2872 (F–NH_2 functionalized), and cuf_1627 (F–OCH_3 functionalized) were identified as the top three membranes for the CH_4/N_2 membrane-based separation with CH_4/N_2 membrane selectivities and CH_4 permeabilities of 5.3, 4.5, and 5.0 and 5.74 × 10^5, 5.47 × 10^5, and 4.51 × 10^5 Barrer, respectively. An apparent geometric commonality of them is their narrow PLDs (around 4–6 Å) and mediocre void fractions (around 0.55–0.60). As the diffusion selectivities of top 20 MOF adsorbents are near 1 (sorbates diffuse at similar rates), the membrane selectivities are governed by the adsorption selectivities. Similarly, the higher CH_4 permeabilities (compared to N_2 permeabilities) are mostly due to higher amounts of CH_4 captured in the membranes.

3.4 N_2/H_2 separation

Fig. S4† illustrates the N_2/H_2 separation performance metrics of the MOFs in tandem with their textural features. The top panels demonstrate that, in general, the more N_2 selective MOFs have higher N_2 working capacities and smaller void fractions. The ranges of N_2/H_2 selectivity, N_2 working

Table 2 20 best MOF adsorbents identified for the CH_4/N_2 separation in tandem with their membrane-based separation performances

Structure	$S_{ads,CH_4/N_2}$	ΔN_{CH_4} (mol kg^{-1})	R_{CH_4} (%)	$S_{diff,CH_4/N_2}$	$S_{mem,CH_4/N_2}$	D_{self,CH_4} (m^2 s^{-1})	D_{self,N_2} (m^2 s^{-1})	P_{CH_4} (Barrer)	P_{N_2} (Barrer)
cuf_2878	4.6	4.5	78.5	1.04	4.8	1.51 × 10^{-8}	1.46 × 10^{-8}	4.59 × 10^5	9.39 × 10^4
cuf_1627	4.7	4.2	80.4	1.05	5.0	1.59 × 10^{-8}	1.51 × 10^{-8}	4.51 × 10^5	8.88 × 10^4
cuf_586	4.5	4.4	78.5	0.97	4.4	1.08 × 10^{-8}	1.11 × 10^{-8}	3.20 × 10^5	7.15 × 10^4
cuf_810	4.7	4.1	79.4	0.83	3.9	7.15 × 10^{-9}	8.59 × 10^{-9}	2.05 × 10^5	5.15 × 10^4
cuf_1633	4.8	4.0	78.6	1.04	5.0	1.14 × 10^{-8}	1.10 × 10^{-8}	3.19 × 10^5	6.26 × 10^4
cuf_811	4.6	4.1	80.8	0.85	3.9	1.01 × 10^{-8}	1.18 × 10^{-8}	2.84 × 10^5	7.13 × 10^4
cuf_735	4.1	4.6	80.5	1.09	4.5	1.77 × 10^{-8}	1.61 × 10^{-8}	4.57 × 10^5	1.01 × 10^5
cuf_818	4.9	4.0	75.8	1.08	5.3	1.87 × 10^{-8}	1.73 × 10^{-8}	5.74 × 10^5	1.06 × 10^5
pMOF_44	4.0	4.4	82.6	0.87	3.5	1.25 × 10^{-8}	1.43 × 10^{-8}	3.36 × 10^5	9.42 × 10^4
cuf_2872	4.4	4.2	79.9	1.02	4.5	1.91 × 10^{-8}	1.87 × 10^{-8}	5.47 × 10^5	1.20 × 10^5
cuf_7134	5.0	3.8	77.2	1.05	5.2	1.17 × 10^{-8}	1.12 × 10^{-8}	3.37 × 10^5	6.34 × 10^4
cuf_809	4.4	4.2	79.7	0.95	4.1	1.68 × 10^{-8}	1.78 × 10^{-8}	4.46 × 10^5	1.06 × 10^5
pMOF_513	3.5	4.8	84.2	0.96	3.4	1.91 × 10^{-8}	2.00 × 10^{-8}	4.56 × 10^5	1.34 × 10^5
cuf_824	5.0	3.9	73.9	0.91	4.5	1.22 × 10^{-8}	1.34 × 10^{-8}	3.75 × 10^5	8.10 × 10^4
cuf_110	4.9	4.1	73.0	0.80	3.9	5.03 × 10^{-9}	6.32 × 10^{-9}	1.51 × 10^5	3.84 × 10^4
cuf_2640	4.2	4.4	79.5	1.06	4.4	1.49 × 10^{-8}	1.41 × 10^{-8}	4.10 × 10^5	9.08 × 10^4
cuf_7812	4.2	4.3	81.5	1.11	4.6	1.00 × 10^{-8}	9.00 × 10^{-9}	2.61 × 10^5	5.54 × 10^4
pMOF_41	3.8	4.5	84.6	0.99	3.7	1.40 × 10^{-8}	1.41 × 10^{-8}	3.46 × 10^5	9.10 × 10^4
cuf_533	4.5	4.1	78.9	0.93	4.1	1.70 × 10^{-8}	1.84 × 10^{-8}	4.78 × 10^5	1.14 × 10^5
cuf_340	4.2	4.3	79.7	0.86	3.6	1.13 × 10^{-8}	1.32 × 10^{-8}	3.11 × 10^5	8.50 × 10^4

This journal is © The Royal Society of Chemistry and IChemE 2022

Mol. Syst. Des. Eng., 2022, 7, 1707–1721 | 1715

capacity, and N_2 regenerability are 2.0–11.7, 0.1–0.5 mol kg^{-1}, and 88.6–90.9%, respectively. Among them, cuf_916 and cuf_110 stand out from the rest with high N_2/H_2 selectivities (11.7 and 11.0) and large N_2 working capacities (~0.4 and ~0.5 mol kg^{-1}). The bottom panels reveal that those highly N_2 selective (and regenerable) MOFs can have significant confinement effects as they possess relatively small PLDs and surface areas. Benchmarking N_2/H_2 separation potentials of MOFs with others above, it can be concluded that the performance–performance or performance–property trends are similar in all gas separations despite having somewhat different ranges. This can be ascribed to different interaction strengths of adsorbates (*i.e.*, varying levels of adsorbate competition due to different LJ parameters, and presence/absence of

quadrupole moment) and slightly different lists of MOFs investigated for each separation as a result of structural filtering.

Fig. 6 depicts the N_2/H_2 separation performance metrics of the MOFs categorized by functional groups. The top left panel shows that bare MOFs are one of the least N_2 selective MOFs while MOFs functionalized with –OCH_3–OCH_3 are the most N_2 selective MOFs on average. However, it is noteworthy that some of the –NH_2 functionalized MOFs (functionalized with –NH_2–NH_2 and –F–NH_2) attain the highest N_2/H_2 selectivities. The top right panel demonstrates that MOFs functionalized with –NH_2–OCH_3 have one of the largest spreads in N_2 working capacities, and the highest mean N_2 working capacities. Considering the extend of N_2 working capacities attained by bare MOFs, this suggests that
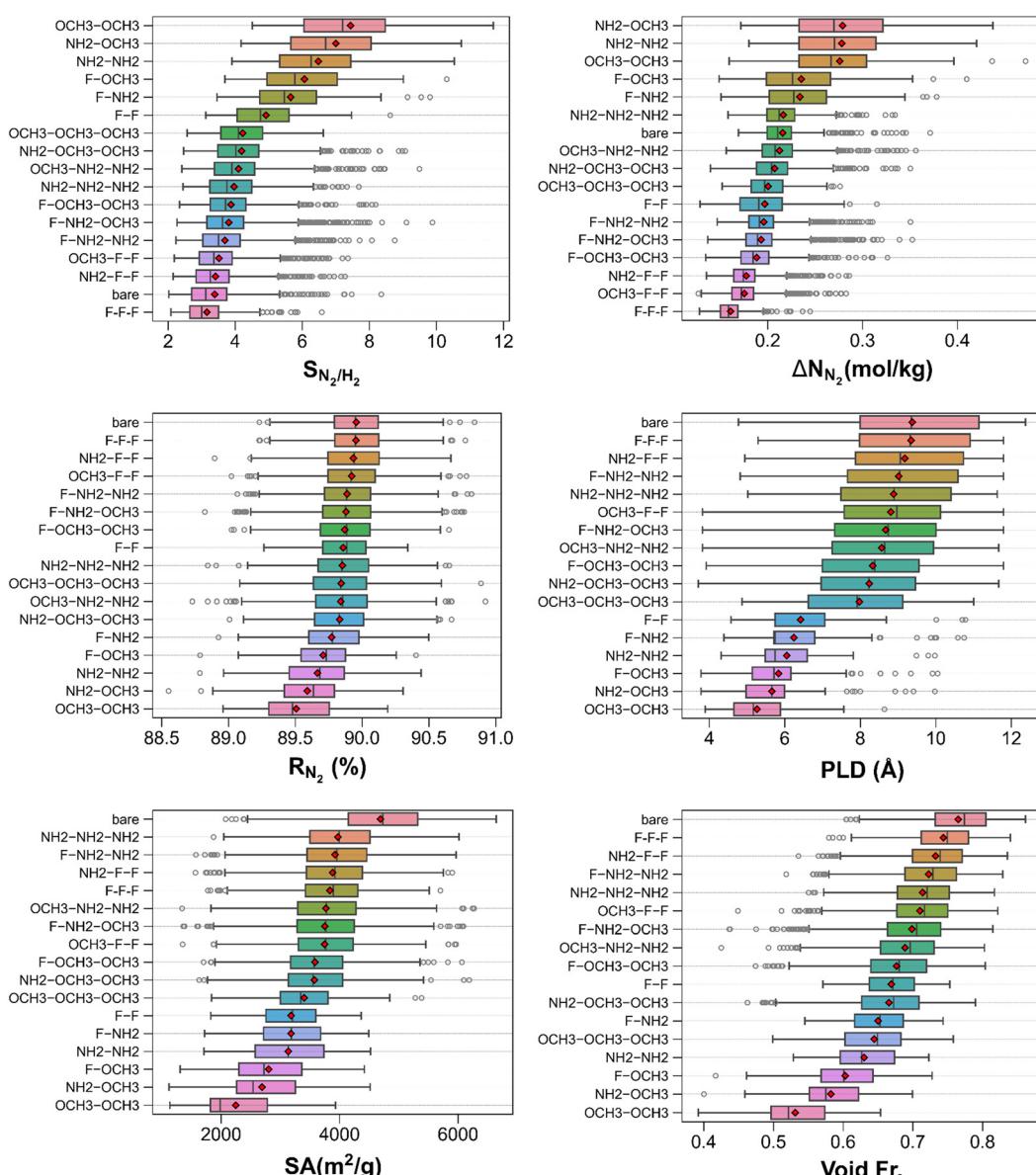
**Fig. 6** Classification of N_2/H_2 separation performance metrics and structural features of MOFs by functional groups.

1716 | *Mol. Syst. Des. Eng.*, 2022, **7**, 1707–1721

This journal is © The Royal Society of Chemistry and IChemE 2022

functionalizing two linkers of bare MOFs can increase the N_2 working capacities considerably. In contrast, MOFs functionalized with –F–F–F show very narrow N_2 working capacity range and the smallest mean N_2 working capacity value hinting that functionalizing all linkers with –F groups is unfavorable for N_2 separation from H_2. It can be deduced from the middle-left panel that all MOF groups attain very similar N_2 regenerabilities on average as well as close minimum/maximum values suggesting that the effect of functionalization on N_2 regenerability is not significant as opposed to that on N_2/H_2 selectivity or N_2 working capacity. The other panels suggest that the textural properties of MOFs used for the N_2/H_2 separation are very similar to those of MOFs probed for the separation of other three gas mixtures.

Table S6† shows the top 20 MOFs for the N_2/H_2 separation whose N_2/H_2 selectivity, N_2 working capacity, and N_2 regenerability span the ranges of 8.9–11.7, 0.4–0.5 mol kg^{-1}, and 88.6–90.0%, respectively. These MOFs have a wide variety of textural properties as evidenced by their PLDs of 3.94–5.74 Å, surface areas of 1136.1–2445.9 m^2 g^{-1}, void fractions of 0.437–0.585, and pore volumes of 0.455–0.711 cm^3 g^{-1}. The best three MOFs are cuf_110, cuf_916, and cuf_824 which are –NH$_2$ and –OCH$_3$ functionalized MOFs (specifically, –OCH$_3$–OCH$_3$, –OCH$_3$–OCH$_3$, and –NH$_2$–OCH$_3$, respectively) attaining N_2/H_2 selectivities of 11.0, 11.7, and 10.7, N_2 working capacities of 0.5, 0.4, and 0.4, and N_2 regenerabilities of 89.0, 89.5, and 89.3%, successively (linker representations for all the top MOFs can be found in Tables S7–S10†).

Having identified the best structures for adsorption and membrane-based separations, we now turn to the performance benchmarks for various types of materials. As for CF$_4$/CH$_4$ separation, the top three adsorbents (pMOF_10, pMOF_26, and pMOF_8) identified in this work exhibit higher CF$_4$/CH$_4$ selectivities and CF$_4$ working capacities than those of top Zr-MOFs reported earlier (up to 5.1 and 2.1 mol kg^{-1}, respectively, at the same conditions as in this work).[15] While the regenerabilities of these MTV-MOFs are less than those of top two Zr-MOFs (72–81% vs. ~84–85%), in practical terms, this may not lead to a significant discrepancy in separation performances as the differences in regenerabilities across top MTV-MOFs and Zr-MOFs are minor. To the best of our knowledge, the top performances (CF$_4$/CH$_4$ selectivity ≥6.0 and CF$_4$ working capacity ≥2.7 mol kg^{-1}) observed in this work imply the highest values reported so far suggesting the potential use of bare MOFs for the CF$_4$/CH$_4$ separation. The higher selectivities of top MTV-MOFs with respect to top Zr-MOFs can be attributed to narrower pore sizes of MTV-MOFs providing tighter CF$_4$ fits. It has been observed that the narrower pores also lead to two-three folds higher adsorption amounts in top MTV-MOFs compared to top Zr-MOFs at the desorption pressure (0.1 bar). At the first glance, this might lead to an impression that MTV-MOFs could not achieve high CF$_4$ working capacities. However, stronger confinement effects together with larger adsorbate–adsorbate interactions in MTV-MOFs lead to significantly different adsorption

amounts (~3.4–4.0 mol kg^{-1} for MTV-MOFs vs. ~2.3–2.8 mol kg^{-1}) at the adsorption pressure (1 bar) leading to ~30–40% higher working capacities.

Comparing the hypothetical MOFs' CH$_4$/H$_2$ separation, it can be inferred that similar adsorption and membrane-based separation performances may be obtained by other MOFs. For instance, in a computational study,[24] the top performing MOF adsorbents (based on adsorbent performance score) were determined to possess CH$_4$/H$_2$ adsorption selectivities of ~25–30 and CH$_4$ working capacities of ~4–6 mol kg^{-1}. In another computational work,[23] an initial MOF membrane screening based on Henry's constants and self-diffusivities calculated at infinite dilution conditions revealed that CH$_4$/H$_2$ membrane selectivities similar to/higher than those reported in this work could be attained. While a large portion of the MOFs have CH$_4$/H$_2$ membrane selectivities between 1 and 10, the highest CH$_4$/H$_2$ adsorption selectivities were above 1000. However, as the effects of presence of multiple sorbate types in materials and higher adsorption pressure were not considered in those calculations, those selectivities could change drastically at the conditions specified in this work.

A recent large-scale screening study[31] on MOFs showed that many MOFs screened in that work have similar or worse CH$_4$/N$_2$ adsorption-based separation performances (CH$_4$/N$_2$ adsorption selectivities between 0.6 and 5, CH$_4$ working capacities up to 4 mol kg^{-1}) than those in the top 20 list of this work. However, they have also identified a few MOFs that can potentially perform better than the hypothetical MOFs studied in this work as they could have CH$_4$/N$_2$ adsorption selectivity larger than 8 or CH$_4$ working capacity bigger than 5 mol kg^{-1}. It is worthwhile to note that those cases also involve trade-offs across at least two metrics (e.g., adsorption selectivity vs. working capacity) and their overall performances may still be comparable to the top adsorbents determined in this work. Yan et al.[30] performed high-throughput screening of computation-ready, experimental (CoRE) MOFs[58] for the CH$_4$/N$_2$ separation around ambient conditions and determined that some of the MOFs can achieve CH$_4$/N$_2$ selectivities ~20. While such selectivities seem much higher than those of top MTV-MOFs identified in this work, it should be reminded that they were attained at a lower adsorption pressure than that in this work (1 vs. 10 bar). While one can typically expect selectivity to drop at higher pressure due to weaker host–guest interactions, it is also possible to observe a cooperative effect between sorbates enhancing the selectivity.[59] Thus, such comparisons should preferably be made after obtaining selectivities at the same pressure conditions.

As to the N_2/H_2 separation, the range of N_2/H_2 adsorption selectivity values (~9–11) might look considerably smaller than those (N_2/H_2 adsorption selectivity up to ~100) reported by Azar et al.[34] However, in the latter work, the competition effects between the sorbates are not considered (infinite dilution conditions) which hinders a one-to-one comparison. While the N_2/H_2 adsorption selectivities of the hypothetical

This journal is © The Royal Society of Chemistry and IChemE 2022

Mol. Syst. Des. Eng., 2022, 7, 1707–1721 | 1717

MOFs investigated in this work are relatively high, the limited N_2 working capacities of the hypothetical MOFs may bring about economic challenges for the selective N_2 removal from H_2.

Before concluding, we would like to note a few aspects of our screening study. Firstly, the MTV-MOF structures obtained from the database[38] were used as they are (*i.e.*, unoptimized structures). It has been shown earlier that structure optimizations (and optimization settings) may lead to considerably different gas uptakes.[60] For instance, it has been shown earlier that while Xe uptake at 298 K, 1 bar in experimentally determined structure of Ni(PyC)$_2$ matches that in one of its optimized counterparts (optimized with unit cell parameter constraints), it is overestimated by other optimized counterpart structures (optimized with unit cell angle constraints and no constraints).[60] Secondly, while the studied gas mixtures are assumed to be dry, in practice, they may include varying levels of humidity which can affect the separation performances (adsorption selectivity, membrane selectivity, gas permeability) of adsorbents and/or membranes.[61] As an example, Daglar *et al.*[61] demonstrated that the inclusion of H_2O in CO_2/N_2 mixture can hamper the adsorption and membrane selectivity together with gas permeabilities. However, as the simulations involving H_2O are typically computationally very expensive, we have not carried out simulations to study separation of humid mixtures. Thirdly, while not considered in this study, the inclusion of framework flexibility in the simulations can be important for adsorption and/or membrane-based separations depending on the case.[62–64] Despite this fact, flexible frameworks were not employed in the simulations as universal and accurate flexible force-field parameters are not available in the literature for a diverse set of materials. Also, as the simulations employing flexible materials typically take much longer time than those with rigid materials, it would not be feasible to carry out simulations for the entire set of materials. It should be noted that the incorporation of flexibility effects does not invariably improve or worsen gas uptakes/selectivities of materials as the separation performances of materials are governed by an interplay of pore size, pore chemistry, and intrinsic flexibility.[65] Thus, the separation performances of top materials identified may enhance or deteriorate at varying levels depending on their pore sizes, chemistry and the extent of their flexibilities. To sum up, our computational exploration of MTV-MOFs has unraveled potentially useful adsorbents and membranes which can serve as the starting point for subsequent experimental and theoretical efforts.

4. Conclusions

In this work, the CF_4/CH_4, CH_4/H_2, CH_4/N_2, and N_2/H_2 separation capabilities of MTV-MOFs were investigated. After filtering the structures based on geometric properties, the resulting list of materials have been studied using GCMC simulations to compute the uptakes of four different gas

mixtures under relevant separation conditions. The top adsorbents identified for each gas separation were found to have distinct properties such as different functional groups, and different ranges of pore size, pore volume *etc.* hinting at the disparate structural needs for different gas separation applications. While many different MTV-MOFs were tested for the adsorption-based separation of CF_4/CH_4 mixture, interestingly, the top three MOFs were found to be bare MOFs. For the adsorption-based separation of CH_4/H_2 and CH_4/N_2 mixtures, MTV-MOFs with specific combinations of $-NH_2$, $-F$, and $-OCH_3$ functional groups (*i.e.*, $-NH_2-NH_2$, $-NH_2-OCH_3$, and $-F-OCH_3$) were determined to have the highest three rankings. Similarly, MTV-MOFs with $-OCH_3-OCH_3$, and $-NH_2-OCH_3$ functional groups ranked as the top three for N_2/H_2 separation. Comparison of adsorption-based separation performances of the MTV-MOFs that we considered in this work with the previously studied MOFs showed that MTV MOFs can outperform the latter in terms of one or more adsorption-based separation performance metrics. Our analysis on top three MOFs indicates that MOFs based on chrysene, pyrene, 2,6-naphthyridine, acetylenedicarboxylic acid (chrysene, 2,6-naphthyridine, and acetylenedicarboxylic acid) can be beneficial for CF_4/CH_4, CH_4/N_2, and N_2/H_2 (CH_4/H_2) separation. For the CF_4/CH_4 separation, it has been observed that many top materials involve pyrazine-based linkers as well. Having determined the top adsorbents, membrane-based separation performances of the top 20 materials for CH_4/H_2 and CH_4/N_2 separations were investigated combining the GCMC and MD results through which it has been deduced that the highest membrane selectivities were attained by MOFs with PLDs of ~5–6 Å and void fractions of ~0.55–0.60. For membrane-based separation of CH_4/H_2 and CH_4/N_2 mixtures, MTV-MOFs with $-F$ $-NH_2$, and $-F-OCH_3$ functional groups demonstrated the best performances in terms of equally weighted membrane selectivity and CH_4 permeability. Overall, our results demonstrated that MTV-MOFs are quite promising for the CF_4/CH_4 adsorption-based separation with the highest CF_4/CH_4 selectivities and CF_4 working capacities reported so far. As for the CH_4/H_2 and CH_4/N_2 separation, MTV-MOFs show similar adsorption and/or membrane-based separation performances with respect to other MOFs investigated. While N_2/H_2 adsorption selectivities of MTV-MOFs studied in this work appear lower than some of those in Azar *et al.*'s work,[34] the former is more relevant and accurate as it involves gas competition effects.

Conflicts of interest

The authors declare no competing financial interest.

Acknowledgements

1718 | *Mol. Syst. Des. Eng.*, 2022, **7**, 1707–1721

This journal is © The Royal Society of Chemistry and IChemE 2022

References

1 C. A. Trickett, A. Helal, B. A. Al-Maythalony, Z. H. Yamani, K. E. Cordova and O. M. Yaghi, The Chemistry of Metal–Organic Frameworks for CO_2 Capture, Regeneration and Conversion, *Nat. Rev. Mater.*, 2017, **2**, 17045.

2 X. Zhao, Y. Wang, D.-S. Li, X. Bu and P. Feng, Metal–Organic Frameworks for Separation, *Adv. Mater.*, 2018, **30**, 1705189.

3 L. Jiao, Y. Wang, H.-L. Jiang and Q. Xu, Metal–Organic Frameworks as Platforms for Catalytic Applications, *Adv. Mater.*, 2018, **30**, 1703663.

4 I. Stassen, N. Burtch, A. Talin, P. Falcaro, M. Allendorf and R. Ameloot, An Updated Roadmap for the Integration of Metal–Organic Frameworks with Electronic Devices and Chemical Sensors, *Chem. Soc. Rev.*, 2017, **46**, 3185–3241.

5 J. Yang and Y.-W. Yang, Metal–Organic Frameworks for Biomedical Applications, *Small*, 2020, **16**, 1906846.

6 J. Li, X. Wang, G. Zhao, C. Chen, Z. Chai, A. Alsaedi, T. Hayat and X. Wang, Metal–Organic Framework-Based Materials: Superior Adsorbents for the Capture of Toxic and Radioactive Metal Ions, *Chem. Soc. Rev.*, 2018, **47**, 2322–2356.

7 K. Adil, Y. Belmabkhout, R. S. Pillai, A. Cadiau, P. M. Bhatt, A. H. Assen, G. Maurin and M. Eddaoudi, Gas/Vapour Separation Using Ultra-Microporous Metal-Organic Frameworks: Insights into the Structure/Separation Relationship, *Chem. Soc. Rev.*, 2017, **46**, 3402–3430.

8 P. Z. Moghadam, A. Li, S. B. Wiggin, A. Tao, A. G. P. Maloney, P. A. Wood, S. C. Ward and D. Fairen-Jimenez, Development of a Cambridge Structural Database Subset: A Collection of Metal–Organic Frameworks for Past, Present, and Future, *Chem. Mater.*, 2017, **29**, 2618–2625.

9 P. G. Boyd, A. Chidambaram, E. García-Díez, C. P. Ireland, T. D. Daff, R. Bounds, A. Gładysiak, P. Schouwink, S. M. Moosavi and M. M. Maroto-Valer, *et al.*, Data-Driven Design of Metal–Organic Frameworks for Wet Flue Gas CO_2 Capture, *Nature*, 2019, **576**, 253–256.

10 Y. G. Chung, E. Haldoupis, B. J. Bucior, M. Haranczyk, S. Lee, H. Zhang, K. D. Vogiatzis, M. Milisavljevic, S. Ling and J. S. Camp, *et al.*, Advances, Updates, and Analytics for the Computation-Ready, Experimental Metal–Organic Framework Database: CoRE MOF 2019, *J. Chem. Eng. Data*, 2019, **64**, 5985–5998.

11 S. W. Choi, D.-H. Lee, J. Kim, J. Kim, J.-H. Park, H. T. Beum, D.-S. Lim and K. B. Lee, A Titanium Carbide-Derived Novel Tetrafluoromethane Adsorbent with Outstanding Adsorption Performance, *Chem. Eng. J.*, 2017, **311**, 227–235.

12 I. Senkovska, E. Barea, J. A. R. Navarro and S. Kaskel, Adsorptive Capturing and Storing Greenhouse Gases Such as Sulfur Hexafluoride and Carbon Tetrafluoride Using Metal–Organic Frameworks, *Microporous Mesoporous Mater.*, 2012, **156**, 115–120.

13 Y. Guo, J. Hu, X. Liu, T. Sun, S. Zhao and S. Wang, Scalable Solvent-Free Preparation of $[Ni_3(HCOO)_6]$ Frameworks for Highly Efficient Separation of CH_4 from N_2, *Chem. Eng. J.*, 2017, **327**, 564–572.

14 S. Calero, J. J. Gutiérrez-Sevillano and E. García-Pérez, Effect of the Molecular Interactions on the Separation of Nonpolar Mixtures Using Cu-BTC Metal–Organic Framework, *Microporous Mesoporous Mater.*, 2013, **165**, 79–83.

15 H. Demir and S. Keskin, Zr-MOFs for CF_4/CH_4, CH_4/H_2, and CH_4/N_2 Separation: Towards the Goal of Discovering Stable and Effective Adsorbents, *Mol. Syst. Des. Eng.*, 2021, **6**, 627–642.

16 M. A. Moreira, R. O. M. Dias, U.-H. Lee, J.-S. Chang, A. M. Ribeiro, A. F. P. Ferreira and A. E. Rodrigues, Adsorption Equilibrium of Carbon Dioxide, Methane, Nitrogen, Carbon Monoxide, and Hydrogen on UiO-66(Zr)_(COOH)₂, *J. Chem. Eng. Data*, 2019, **64**, 4724–4732.

17 Z. Chen, P. Li, R. Anderson, X. Wang, X. Zhang, L. Robison, L. R. Redfern, S. Moribe, T. Islamoglu and D. A. Gómez-Gualdrón, *et al.*, Balancing Volumetric and Gravimetric Uptake in Highly Porous Materials for Clean Energy, *Science*, 2020, **368**, 297–303.

18 M. D. Allendorf, Z. Hulvey, T. Gennett, A. Ahmed, T. Autrey, J. Camp, E. Seon Cho, H. Furukawa, M. Haranczyk and M. Head-Gordon, *et al.*, An Assessment of Strategies for the Development of Solid-State Adsorbents for Vehicular Hydrogen Storage, *Energy Environ. Sci.*, 2018, **11**, 2784–2812.

19 B. Liu, Q. Yang, C. Xue, C. Zhong, B. Chen and B. Smit, Enhanced Adsorption Selectivity of Hydrogen/Methane Mixtures in Metal–Organic Frameworks with Interpenetration: A Molecular Simulation Study, *J. Phys. Chem. C*, 2008, **112**, 9854–9860.

20 M. Gallo and D. Glossman-Mitnik, Fuel Gas Storage and Separations by Metal–Organic Frameworks: Simulated Adsorption Isotherms for H_2 and CH_4 and Their Equimolar Mixture, *J. Phys. Chem. C*, 2009, **113**, 6634–6642.

21 S. Qiu, M. Xue and G. Zhu, Metal–Organic Framework Membranes: From Synthesis to Separation Application, *Chem. Soc. Rev.*, 2014, **43**, 6116–6140.

22 H. Daglar and S. Keskin, Recent Advances, Opportunities, and Challenges in High-Throughput Computational Screening of MOFs for Gas Separations, *Coord. Chem. Rev.*, 2020, **422**, 213470.

23 C. Altintas, G. Avci, H. Daglar, E. Gulcay, I. Erucar and S. Keskin, Computer Simulations of 4240 MOF Membranes for H_2/CH_4 Separations: Insights into Structure–Performance Relations, *J. Mater. Chem. A*, 2018, **6**, 5836–5847.

24 C. Altintas, I. Erucar and S. Keskin, High-Throughput Computational Screening of the Metal Organic Framework Database for CH_4/H_2 Separations, *ACS Appl. Mater. Interfaces*, 2018, **10**, 3668–3679.

25 T.-H. Kim, S.-Y. Kim, T.-U. Yoon, M.-B. Kim, W. Park, H. H. Han, C. Kong, C.-Y. Park, J.-H. Kim and Y.-S. Bae, Improved

This journal is © The Royal Society of Chemistry and IChemE 2022

Mol. Syst. Des. Eng., 2022, **7**, 1707–1721 | 1719

Methane/Nitrogen Separation Properties of Zirconium-Based Metal–Organic Framework by Incorporating Highly Polarizable Bromine Atoms, *Chem. Eng. J.*, 2020, **399**, 125717.

26 X. Wu, B. Yuan, Z. Bao and S. Deng, Adsorption of Carbon Dioxide, Methane and Nitrogen on an Ultramicroporous Copper Metal–Organic Framework, *J. Colloid Interface Sci.*, 2014, **430**, 78–84.

27 J. Hu, T. Sun, X. Liu, Y. Guo and S. Wang, Separation of CH_4/N_2 Mixtures in Metal–Organic Frameworks with 1D Micro-Channels, *RSC Adv.*, 2016, **6**, 64039–64046.

28 J. Hu, T. Sun, X. Liu, S. Zhao and S. Wang, Rationally Tuning the Separation Performances of $[M_3(HCOO)_6]$ Frameworks for CH_4/N_2 Mixtures via Metal Substitution, *Microporous Mesoporous Mater.*, 2016, **225**, 456–464.

29 Z. Sumer and S. Keskin, Adsorption- and Membrane-Based CH_4/N_2 Separation Performances of MOFs, *Ind. Eng. Chem. Res.*, 2017, **56**, 8713–8722.

30 T. Yan, Y. Lan, D. Liu, Q. Yang and C. Zhong, Large-Scale Screening and Design of Metal–Organic Frameworks for CH_4/N_2 Separation, *Chem. - Asian J.*, 2019, **14**, 3688–3693.

31 H. C. Gulbalkan, Z. P. Haslak, C. Altintas, A. Uzun and S. Keskin, Assessing CH_4/N_2 Separation Potential of MOFs, COFs, IL/MOF, MOF/Polymer, and COF/Polymer Composites, *Chem. Eng. J.*, 2021, 131239.

32 B. Mu, P. M. Schoenecker and K. S. Walton, Gas Adsorption Study on Mesoporous Metal–Organic Framework UMCM-1, *J. Phys. Chem. C*, 2010, **114**, 6464–6471.

33 M. J. Regufe, J. Tamajon, A. M. Ribeiro, A. Ferreira, U.-H. Lee, Y. K. Hwang, J.-S. Chang, C. Serre, J. M. Loureiro and A. E. Rodrigues, Syngas Purification by Porous Amino-Functionalized Titanium Terephthalate MIL-125, *Energy Fuels*, 2015, **29**, 4654–4664.

34 A. N. V. Azar, S. Velioglu and S. Keskin, Large-Scale Computational Screening of Metal Organic Framework (MOF) Membranes and MOF-Based Polymer Membranes for H_2/N_2 Separations, *ACS Sustainable Chem. Eng.*, 2019, **7**, 9525–9536.

35 A. Kirchon, L. Feng, H. F. Drake, E. A. Joseph and H.-C. Zhou, From Fundamentals to Applications: A Toolbox for Robust and Multifunctional MOF Materials, *Chem. Soc. Rev.*, 2018, **47**, 8611–8638.

36 Y.-B. Zhang, H. Furukawa, N. Ko, W. Nie, H. J. Park, S. Okajima, K. E. Cordova, H. Deng, J. Kim and O. M. Yaghi, Introduction of Functionality, Selection of Topology, and Enhancement of Gas Adsorption in Multivariate Metal–Organic Framework-177, *J. Am. Chem. Soc.*, 2015, **137**, 2641–2650.

37 Z. Hu, A. Gami, Y. Wang and D. Zhao, A Triphasic Modulated Hydrothermal Approach for the Synthesis of Multivariate Metal–Organic Frameworks with Hydrophobic Moieties for Highly Efficient Moisture-Resistant CO_2 Capture, *Adv. Sustainable Syst.*, 2017, **1**, 1700092.

38 S. Li, Y. G. Chung, C. M. Simon and R. Q. Snurr, High-Throughput Computational Screening of Multivariate Metal–Organic Frameworks (MTV-MOFs) for CO_2 Capture, *J. Phys. Chem. Lett.*, 2017, **8**, 6135–6141.

39 T. F. Willems, C. H. Rycroft, M. Kazi, J. C. Meza and M. Haranczyk, Algorithms and Tools for High-Throughput Geometry-Based Analysis of Crystalline Porous Materials, *Microporous Mesoporous Mater.*, 2012, **149**, 134–141.

40 D. Ongari, P. G. Boyd, S. Barthel, M. Witman, M. Haranczyk and B. Smit, Accurate Characterization of the Pore Volume in Microporous Crystalline Materials, *Langmuir*, 2017, **33**, 14529–14538.

41 E. Haldoupis, S. Nair and D. S. Sholl, Efficient Calculation of Diffusion Limitations in Metal Organic Framework Materials: A Tool for Identifying Materials for Kinetic Separations, *J. Am. Chem. Soc.*, 2010, **132**, 7528–7539.

42 D. Dubbeldam, S. Calero, D. E. Ellis and R. Q. Snurr, RASPA: Molecular Simulation Software for Adsorption and Diffusion in Flexible Nanoporous Materials, *Mol. Simul.*, 2016, **42**, 81–101.

43 M. Heuchel, R. Q. Snurr and E. Buss, Adsorption of CH_4–CF_4 Mixtures in Silicalite: Simulation, Experiment, and Theory, *Langmuir*, 1997, **13**, 6795–6804.

44 I. Erucar and S. Keskin, Computational Assessment of MOF Membranes for CH_4/H_2 Separations, *J. Membr. Sci.*, 2016, **514**, 313–321.

45 D. Wu, C. Wang, B. Liu, D. Liu, Q. Yang and C. Zhong, Large-Scale Computational Screening of Metal-Organic Frameworks for CH_4/H_2 Separation, *AIChE J.*, 2012, **58**, 2078–2084.

46 O. C. David, D. Gorri, K. Nijmeijer, I. Ortiz and A. Urtiaga, Hydrogen Separation from Multicomponent Gas Mixtures Containing CO, N_2 and CO_2 Using Matrimid® Asymmetric Hollow Fiber Membranes, *J. Membr. Sci.*, 2012, **419–420**, 49–56.

47 M. A. Nadeem, A. W. Thornton, M. R. Hill and J. A. Stride, A Flexible Copper Based Microporous Metal–Organic Framework Displaying Selective Adsorption of Hydrogen over Nitrogen, *Dalton Trans.*, 2011, **40**, 3398–3401.

48 S.-H. Choi, A. Brunetti, E. Drioli and G. Barbieri, H_2 Separation From H_2/N_2 and H_2/CO Mixtures with Co-Polyimide Hollow Fiber Module, *Sep. Sci. Technol.*, 2010, **46**, 1–13.

49 A. K. Rappe, C. J. Casewit, K. S. Colwell, W. A. Goddard and W. M. Skiff, UFF, a Full Periodic Table Force Field for Molecular Mechanics and Molecular Dynamics Simulations, *J. Am. Chem. Soc.*, 1992, **114**, 10024–10035.

50 S. Kancharlapalli, A. Gopalan, M. Haranczyk and R. Q. Snurr, Fast and Accurate Machine Learning Strategy for Calculating Partial Atomic Charges in Metal–Organic Frameworks, *J. Chem. Theory Comput.*, 2021, **17**, 3052–3064.

51 A. I. Skoulidas, T. C. Bowen, C. M. Doelling, J. L. Falconer, R. D. Noble and D. S. Sholl, Comparing Atomistic Simulations and Experimental Measurements for CH_4/CF_4 Mixture Permeation through Silicalite Membranes, *J. Membr. Sci.*, 2003, **227**, 123–136.

52 M. G. Martin and J. I. Siepmann, Transferable Potentials for Phase Equilibria. 1. United-Atom Description of n-Alkanes, *J. Phys. Chem. B*, 1998, **102**, 2569–2577.

53 J. J. Potoff and J. I. Siepmann, Vapor–Liquid Equilibria of Mixtures Containing Alkanes, Carbon Dioxide, and Nitrogen, *AIChE J.*, 2001, **47**, 1676–1682.

1720 | *Mol. Syst. Des. Eng.*, 2022, **7**, 1707–1721

This journal is © The Royal Society of Chemistry and IChemE 2022

54 V. Buch, Path Integral Simulations of Mixed Para-D_2 and Ortho-D_2 Clusters: The Orientational Effects, *J. Chem. Phys.*, 1994, **100**, 7610–7629.

55 P. P. Ewald, The Calculation of Optical and Electrostatic Grid Potential, *Ann. Phys.*, 1921, **64**, 253–287.

56 D. Frenkel and B. Smit, *Understanding Molecular Simulation: From Algorithms to Applications*, Academic Press, San Diego, CA, 2002.

57 A. Einstein, *Investigations on the Theory of the Brownian Movement*, Courier Corporation, New York, 1956.

58 Y. G. Chung, J. Camp, M. Haranczyk, B. J. Sikora, W. Bury, V. Krungleviciute, T. Yildirim, O. K. Farha, D. S. Sholl and R. Q. Snurr, Computation-Ready, Experimental Metal–Organic Frameworks: A Tool To Enable High-Throughput Screening of Nanoporous Crystals, *Chem. Mater.*, 2014, **26**, 6185–6192.

59 E. Ren and F.-X. Coudert, Thermodynamic Exploration of Xenon/Krypton Separation Based on a High-Throughput Screening, *Faraday Discuss.*, 2021, **231**, 201–223.

60 N. Gantzler, M.-B. Kim, A. Robinson, M. W. Terban, S. Ghose, R. E. Dinnebier, A. H. York, D. Tiana, C. M. Simon and P. K. Thallapally, Computation-Informed Optimization of Ni(PyC)2 Functionalization for Noble Gas Separations, *ChemRxiv*, 2021, preprint, DOI: **10.26434/chemrxiv-2021-sr171**.

61 H. Daglar and S. Keskin, Computational Screening of Metal–Organic Frameworks for Membrane-Based $CO_2/N_2/H_2O$ Separations: Best Materials for Flue Gas Separation, *J. Phys. Chem. C*, 2018, **122**, 17347–17357.

62 Z. Yu, D. M. Anstine, S. E. Boulfelfel, C. Gu, C. M. Colina and D. S. Sholl, Incorporating Flexibility Effects into Metal–Organic Framework Adsorption Simulations Using Different Models, *ACS Appl. Mater. Interfaces*, 2021, **13**, 61305–61315.

63 C. Altintas and S. Keskin, Molecular Simulations of MOF Membranes and Performance Predictions of MOF/Polymer Mixed Matrix Membranes for CO_2/CH_4 Separations, *ACS Sustainable Chem. Eng.*, 2019, **7**, 2739–2750.

64 I. Erucar and S. Keskin, Computational Modeling of Bio-MOFs for CO_2/CH_4 Separations, *Chem. Eng. Sci.*, 2015, **130**, 120–128.

65 M. Witman, S. Ling, S. Jawahery, P. G. Boyd, M. Haranczyk, B. Slater and B. Smit, The Influence of Intrinsic Framework Flexibility on Adsorption in Nanoporous Materials, *J. Am. Chem. Soc.*, 2017, **139**, 5547–5557.

66 O. F. Altundal, Z. P. Haslak and S. Keskin, *Ind. Eng. Chem. Res.*, 2021, **60**(35), 12999–13012.

67 Y. Lim and J. Kim, *Mol. Syst. Des. Eng.*, 2022, **7**, 1056–1064.

This journal is © The Royal Society of Chemistry and IChemE 2022

Mol. Syst. Des. Eng., 2022, **7**, 1707–1721 | 1721